

ORIGINAL ARTICLE

# Recurrent internal waves in a small lake: Potential ecological consequences for metalimnetic phytoplankton populations

Alexandrine Pannard,<sup>1,2</sup> Beatrix E. Beisner,<sup>1</sup> David F. Bird,<sup>1</sup> Jean Braun,<sup>3</sup> Dolores Planas,<sup>1</sup>  
and Myriam Bormans<sup>4</sup>

## Abstract

Worldwide, small lakes (< 1 km<sup>2</sup>) are numerically dominant, yet the potential for interaction between physical and ecological processes therein has been largely ignored. High-frequency time series of the thermal and current structures in a small dimictic lake (Lake Bromont, Quebec) revealed the occurrence of recurrent internal waves during the summer of 2007. Amplitudes and frequencies of the internal wave modes were characterized, along with wind and stratification conditions, during two focal periods of 5 days at the beginning and the end of the summer. Owing to a resonance with the daily wind, the second and third vertical mode seiches dominated over the first mode, which was observed only during larger wind events. Although the lake is small (0.41 km<sup>2</sup>) and shallow (mean depth of 4 m), the response of the thermal structure of the lake to wind forcing was very similar to that of alpine and other deep lakes. The phytoplankton community was controlled by the contrasting gradients of light and nutrients. Consequently, metalimnetic communities of cyanobacteria exposed to the recurrent internal waves, which occurred throughout the summer, formed the dominant phytoplankton biomass in the lake. The regular vertical excursion of the metalimnion influenced both light availability and nutrient fluxes and most likely contributed to an enhanced algal biomass.

Keywords: cyanobacteria, light climate, nutrients, wind

## Introduction

[1] Worldwide, most lakes are small and have a surface area smaller than 1 km<sup>2</sup>. About 99.8% (300 million) of these lakes constitute 43.3% of the total lake surface area (Downing et al. 2006). The same is true on a regional scale, for example, in Sweden (97.6%; Håkanson and Lindstrom 1997) and in Quebec, Canada (77%; based on data from a total of 1843 lakes; T. L. Sauteur, pers. comm.). Hanson et al. (2007) showed that the exclusion of small lakes in

regional characterization of water quality can misrepresent global organic and inorganic carbon concentrations. Understanding the ecological processes in small lakes is therefore of great importance in many regions, including northeastern and central North America, yet small lakes remain relatively understudied (Scheffer 2001), especially with respect to lake physics. Interestingly, the consequences of physics on ecological processes may be magnified in small lakes due to a greater boundary effect

<sup>1</sup>Groupe de Recherche Inter-universitaire en Limnologie, Département des sciences biologiques, Université du Québec à Montréal, Montréal, Québec, Canada

<sup>2</sup>Present address: Unité Mixte de Recherche (UMR) 6553, Centre National de Recherche Scientifique (CNRS), Institut Fédératif de Recherche – Centre Armoricain de Recherche en Environnement (IFR CAREN), Université de Rennes 1, Rennes, France

<sup>3</sup>Université Joseph Fourier, Grenoble, France

<sup>4</sup>UMR 6553, CNRS, IFR CAREN, Université de Rennes 1, Rennes, France

Correspondence to  
Alexandrine Pannard,  
alexandrine.pannard@  
univ-rennes1.fr

because the ratio between the benthic boundary layer (BBL) and the volume of the pelagic zone is higher. Physical processes and ecological functioning in small lakes have mainly been studied in shallow systems, through examination of the effects of wind-induced surface waves on sediment resuspension (Cozar et al. 2005), phosphorus concentration (Søndergaard et al. 1992), and phytoplankton communities (Carrick et al. 1993; Schallenberg and Burns 2004). The effects of wind-induced internal waves have been largely ignored, despite the fact that small lakes can exhibit persistent stratification yet may be susceptible to low Lake number. The Lake number is a dimensionless number that represents the ratio of the stabilizing gravity force associated with density stratification to the destabilizing forces associated with wind forcing and mixing (Robertson and Imberger 1994).

[2] Wind-induced internal waves, also called *seiches*, have been recognized since the 1950s (Mortimer 1953), predominantly in lakes of large and intermediate depth and size. Even though internal waves are a ubiquitous feature of both lakes and oceans, their occurrence in small lakes has seldom been studied (LaZerte 1980), and their ecological consequences have received even less attention. In small lakes, a restricted surface area limits the interface through which wind kinetic energy can be transferred to a lake, resulting generally in weaker mixing and shallower thermoclines (Rueda-Valdivia and Schladow 2009). To our knowledge, the smallest and shallowest lake for which internal waves have been reported is Lake Frain (Michigan), which has a surface area of only 0.07 km<sup>2</sup> and a maximum depth of 9.1 m (LaZerte 1980). Given the potential for internal waves in small lakes, it is relevant to determine whether such physical processes are important for ecological functioning.

[3] Recent research has addressed the interaction between physical forcing and biological responses, including phytoplankton photosynthesis (Evans et al. 2008), the occurrence of harmful algal blooms (Jöhnk et al. 2008), and the distribution and abundance of plankton (Rinke et al. 2007). Many ecological processes in lakes, including nutrient fluxes (MacIntyre et al. 1999, 2006) and biomass losses by sedimentation (Diehl 2002), are influenced by the vertical structure of the water column and wind-associated mixing (Imberger

and Parker 1985). Internal waves can increase nutrient inputs from the hypolimnion to the epilimnion (MacIntyre and Jellison 2001; Bormans et al. 2004) and thereby influence phytoplankton community composition during periods of extended stratification (Beisner 2001; Pannard et al. 2008). Internal waves can increase primary production by affecting light availability for photosynthetic bacteria and phytoplankton (Evans et al. 2008; Rimmer et al. 2008). During seiches, the turbulent BBL, in particular, plays a major role in mass transport processes (e.g., nutrient diffusion), with intrusions from the slope of the basin or lake boundaries to the center of the lake (MacIntyre et al. 1999). In lakes with a thin hypolimnion, mixing in the metalimnion near the bottom of the lake and in the littoral zone is enhanced as kinetic energy introduced by wind at the water surface is transferred to internal waves (Münnich et al. 1992). Nutrient fluxes, as well as resuspension of sediment and phytoplankton cells, have been shown in large stratified lakes to influence the ecology and, in particular, to increase phytoplankton biomass in shallow littoral zones (Ostrovsky et al. 1996). Such ecological effects remain to be demonstrated in smaller lakes, where their effects should be amplified, as mentioned previously.

[4] The first objective of this study was to characterize the amplitudes and frequencies of internal waves during a stratified summer period in a small lake. The second objective was to test the hypothesis that phytoplankton populations, which developed at depths close to these internal waves, gain an ecological advantage when they are located in these turbulent metalimnetic layers. Overall, our goal was to determine the potential consequences for resource (light and nutrient) availability and photosynthetic activity of the metalimnetic phytoplankton community in a small lake exposed to internal waves.

## Methods

### *Study Site*

[5] Lake Bromont is located in the Eastern Townships region of Quebec (Canada), in one of the Monteregian Hills, Mont Brome (maximum altitude, 553 m). Mont Brome is bisected by an east–west valley, so Lake Bromont is directly exposed to westerly wind and protected from northern winds. The steep-sided basin of the lake,

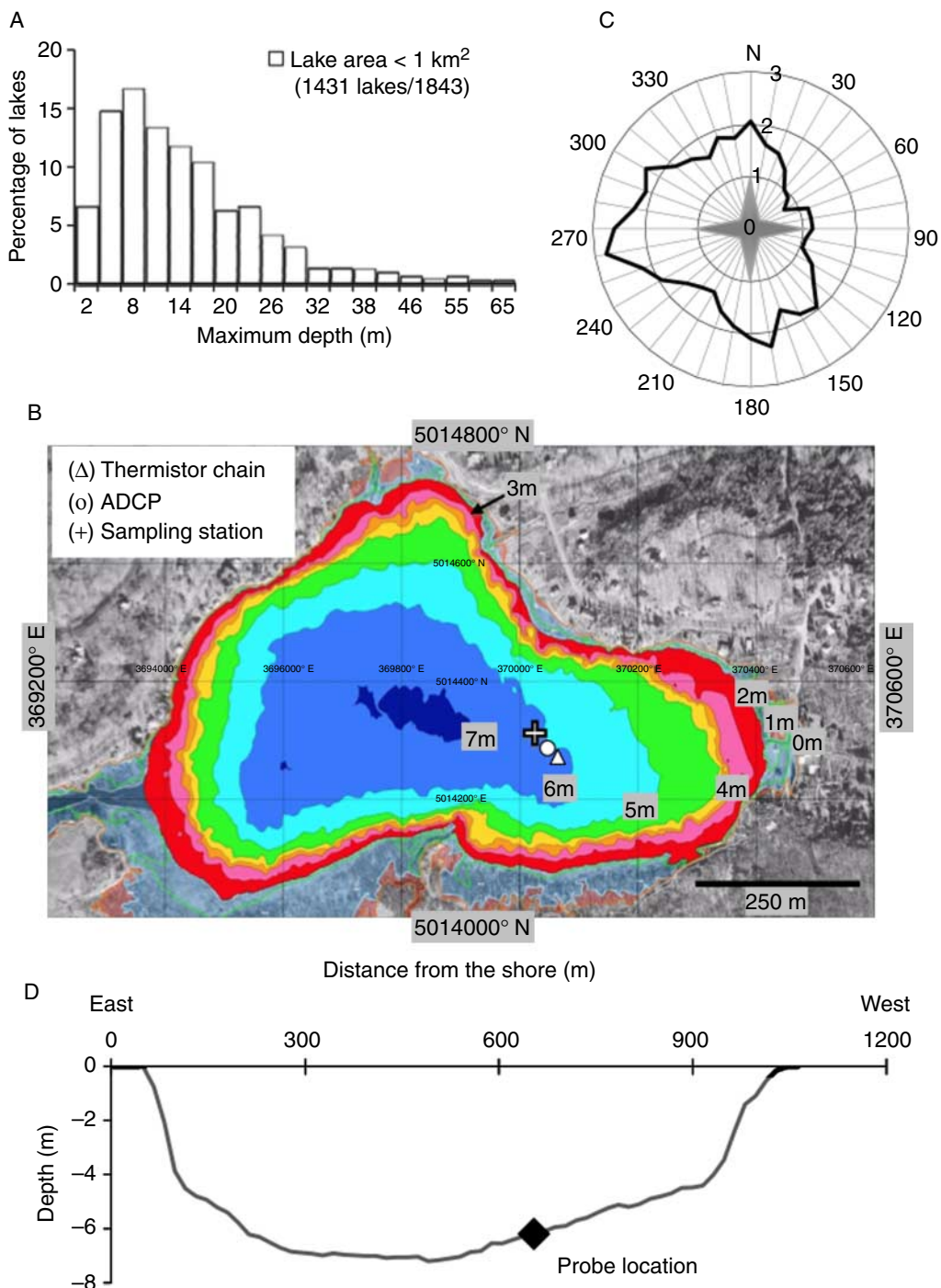


**Fig. 1** (A) Depth distribution of 1431 lakes in Quebec (T. L. Sauteur, pers. comm.) with a surface area less than 1 km<sup>2</sup>. (B) Bathymetric map of Lake Bromont (McMeekin 2009), indicating the location of the thermistor chain, the Acoustic Doppler Current Profiler (ADCP), and the sampling station for chemical and biological parameters. All three sites were within 10 m of each other. (C) Wind rose showing wind direction and velocity (m s<sup>-1</sup>) from hourly data between 1 June and 30 September 2007 (Environment Canada 2007). (D) Bathymetric profile of the lake crossing the deepest station, along the axis of dominant winds.

exposed to the direction of dominant westerly winds, likely contributes to a funnel effect. The surface area of the lake is 0.45 km<sup>2</sup> (mean depth of 4 m and maximum depth of 7.2 m), within a drainage area of 23.47 km<sup>2</sup> (Fig. 1B).

#### Meteorological Data

[6] Data for the summer of 2007 were obtained from the meteorological station at Frelighsburg, 25 km southwest (Environment Canada 2007). Solar radiation data, wind speed, and direction were monitored hourly, and rainfall, mean, and maximum air temperatures were recorded daily. Solar radiation data, which were compared with in situ photosynthetically active radiation (PAR) values (see below), had a high correlation ( $r = 0.98$ ). A correction factor for winds at Frelighsburg was inferred by comparing these winds to values measured by a meteorological station on the lake from mid-July to mid-September 2009 (Fig. 1C). Hourly means in westerly wind velocity measured locally were higher than those measured in Frelighsburg ( $r = 0.73$ ;  $n = 1506$ ; data not shown), probably due to topographic steering. Local wind disturbances were thus characterized through surface current velocity increases, as this estimated the direct lake response to wind forcing.

#### Physical Data Collection

[7] An Acoustic Doppler Current Profiler (ADCP) and a thermistor chain were deployed from 2 May to 27 September 2007 near the deepest point of the lake (Fig. 1). The ADCP (Argonaut XR, 1500 kHz; Sontek/YSI Environmental, Yellow Springs, OH, USA) measured horizontal and vertical current velocities every 20 min with three consecutive pulses (burst mode) in 10 vertical cells of 0.6 m depth, and changes in water level (0.1 m accuracy), which remained  $< 0.2$  m during the two focal periods (see below) and  $< 0.3$  m throughout the summer. The thermistor chain consisted of 10 HOBO Temp Pro Loggers ( $\pm 0.2^\circ\text{C}$  accuracy) placed every 50 cm, from 1 m below the water surface to 0.5 m from the bottom, with sampling frequency of 10 min.

#### Data Treatment: Wind Mixing

[8] The effect of wind on the thermal structure was characterized through the Lake number,  $L_N$ . While

$L_N < 1$  indicates a fully mixed water column,  $L_N \sim 1$  indicates some upwelling of hypolimnetic waters (Robertson and Imberger 1994). Values of  $L_N$  between 1 and 12 are characteristic of internal waves, and  $L_N > 12$  indicates calm, stably stratified conditions (MacIntyre et al. 2006).  $L_N$  was calculated daily using the formula (Imberger and Patterson 1989)

$$L_N = \frac{S_t(H - h_t)}{(u_*^2 A_S^{3/2} (H - h_v))}, \quad (1)$$

where  $S_t$  is the Schmidt stability (see below),  $H$  is the total depth,  $h_t$  is the height from the bottom of the lake to the thermocline,  $h_v$  is the height of the center of lake volume, and  $A_S$  is the surface area of the lake. The shear velocity  $u_*$  due to winds is given by

$$u_* = U \sqrt{C_D^S \rho_a / \rho_o}, \quad (2)$$

where  $U$  is the wind speed at a height of 10 m ( $\text{m s}^{-1}$ ),  $\rho_a$  is air density,  $\rho_o$  is the average density of water, and  $C_D^S$  is the drag coefficient ( $1.3 \times 10^{-3}$ ) (Imberger and Patterson 1989).

#### Stratification Intensity and Stability of the Water Column

[9] Water column stability was inferred from the Schmidt formulation ( $\text{J m}^{-2}$ ),  $S_t$  (Imberger and Patterson 1989), given by

$$S_t = \int_0^H g(h_v - z) \rho_z A_z dz / \rho_o, \quad (3)$$

where  $g$  is the gravitational constant and  $A_z$  and  $\rho_z$  are the area of the lake and the density of water at depth  $z$ . The Schmidt stability was calculated from the thermal distribution every 10 min and then averaged daily.

[10] We analyzed overall patterns of the thermal structure and velocity in the lake for the summer, as well as the short-term variability for two 5-day focal periods with contrasting physical conditions (4–18 June 2007 and 15–19 August 2007). We characterized the internal waves through assessment of the power spectral density of winds, currents, and water temperature, using a two-dimensional model. We related the changes in physical conditions to biologically relevant variables measured over the summer and explored the potential effect of internal waves on primary production.

### Power Spectral Density

[11] To highlight the evolution of periodicities in wind forcing and in the physical response of the lake, spectral densities were calculated for both focal periods for westerly wind speed (dominant direction; see below), for surface (30 cm depth) eastward current velocity, and for temperature at different depths.

### Seiche Periods and Modes

[12] Internal seiches can be distinguished by nodal points on the vertical (V) and horizontal (H) components,  $VnHm$ , where  $n$  and  $m$  represent the number of nodes of each component, thus characterizing the mode. Only the first horizontal modes were considered given the small lake size (Fig. 2). Theoretical periods for the different seiche modes were calculated using a two-dimensional numerical model with continuous

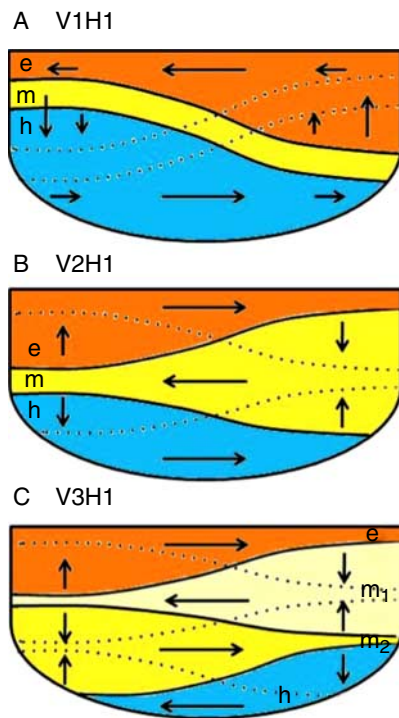


**Fig. 2** Schematic view of the structure of various first horizontal mode internal waves: (A) first vertical mode V1H1, (B) second vertical mode V2H1, and (C) third vertical mode V3H1. The two states of maximum vertical displacement are shown—the first one by solid lines and the second one by dashed lines. Vertical and horizontal arrows show the direction of flow between the first and the second states. Epilimnion (e), metalimnion (m), and hypolimnion (h) are shown, with two metalimnetic layers ( $m_1$ , and  $m_2$ ) in V3H1.

stratification and topography (Fricker and Nepf 2000). Internal wave solutions were calculated for the real bathymetry along the dominant wind axis (Fig. 1D), using observed stratification averaged over each focal period.

[13] The internal seiche solutions were calculated using a finite element discretization of the governing equation, after neglecting nonlinear terms, given by

$$N^2\Psi_{xx} = w^2 \left( \frac{\Psi_{zz} - N^2\Psi_z}{g + \Psi_{xx}} \right), \quad (4)$$

where  $\Psi$  is the stream function,  $w$  is the seiche frequency, and  $N$  is the buoyancy frequency, to generate a generalized eigenvalue problem of the form  $\mathbf{N}\psi = w^2\mathbf{M}\psi$ , which was solved using the `rgg.f` routine described by Press et al. (1992). We used triangular elements in which the solution  $\Psi$  is assumed to vary linearly. The computational mesh was made of 1346 nodes connected by 2547 elements. The mean vertical and horizontal spacing between two nodes were 0.25 m and 16 m, respectively. We imposed  $\Psi = 0$  on all boundaries, assuming also a rigid lid. The analytical solutions (Turner 1973) were also calculated for each seiche mode, considering a rectangular basin (length  $L = 1100$  m  $\times$  total depth  $H = 8$  m) and constant  $N^2$ , in which the horizontal and vertical numbers,  $n$  and  $m$ , are related to the frequency by

$$w_{nm}^2 = \frac{n^2}{(n^2 + (H/L)^{-2}m^2 + (N^4L^2/4\pi^2g^2))}. \quad (5)$$

[14] The resulting seiche periods were compared with the analytical solutions and with the observed periods corresponding to the maximum spectral density in the temperature power spectra. Time series of isotherms were used to identify the internal mode seiche and the phase shifts between different depths. Deviation from daily mean temperature at two metalimnetic depths was also used to highlight coherence in temperature changes between two layers with fluctuations in phase, indicating a first vertical mode, and fluctuations in opposite phase, indicating a second or higher mode. The amplitude of the vertical displacement was calculated from the isotherms.

### Chemical and Biological Parameters

[15] Measurements of the chemical and biological parameters were carried out between May and October at sampling intervals varying between 2 days and 2 weeks, and more frequently in August and September 2007 (Table 1).

[16] Instantaneous PAR profiles were measured three times on each of the 15 sampling dates, at 1-m intervals, with two quantum sensors, a submersible  $4\pi$  sensor (LICOR LI-193SA, Lincoln, NE, USA) for in situ light and a  $2\pi$  sensor (LICOR LI-190SA) for incident light. The light extinction coefficient  $K_d$  was calculated from the Beer-Lambert law. Nutrient concentrations were measured in triplicate at 2.5 m and 5.5 m on June sampling dates and at every 1 m in August and September 2007. Total dissolved phosphorus (TDP) and nitrogen (TDN) and total particulate phosphorus and nitrogen were analyzed according to Cattaneo and Prairie (1995). We calculated the vertical fluxes of P and N available for phytoplankton cells in the metalimnion, using the nutrient profiles, under two scenarios: (1) the minimum fluxes by considering only molecular diffusion, with a vertical eddy diffusion coefficient  $K_z = 1.4 \times 10^{-7} \text{ m}^2 \text{ s}^{-1}$  (Heinz et al. 1990); and (2) estimated turbulent fluxes by considering  $K_z = 2 \times 10^{-5} \text{ m}^2 \text{ s}^{-1}$ , similar to other systems with internal waves (Imberger 1998; MacIntyre et al. 1999; Bormans et al. 2004). Dissolved oxygen (DO) and fluorescence profiles were measured every 0.5 m with a YSI Environmental (San Diego, CA, USA) probe 6920 and a fluoroprobe

(bbe Moldaenke GmbH, Kiel-Kronshagen, Germany), respectively.

[17] The phytoplankton community was vertically structured with a deep chlorophyll maximum (DCM) located at 5 m depth. To characterize photosynthetic parameters of this metalimnetic community, gross photosynthetic oxygen production was measured on each of the 15 sampling dates (Table 1), through in situ incubations between 10:00 h and 15:00 h at three depths (2, 3.5, and 5 m) corresponding to different light intensities (Carignan et al. 2000). Fifteen clear and six dark glass biochemical oxygen demand bottles (300 mL) were filled with water collected at 5 m. DO was measured initially and after incubation using a DO meter (YSI 5100 and YSI 5905-W; YSI Environmental). The net primary production of oxygen (NP) and community respiration (R) were measured from changes in DO in clear and dark bottles. Gross primary production was calculated as  $\text{NP} + \text{R}$  (Carignan et al. 1998), assuming the same respiration between light and dark incubations. Chlorophyll *a* (Chl *a*) was measured by spectrophotometry after extraction with 95% hot ethanol (Sartory and Grobbelaar 1984).

[18] The relationship between productivity and incident irradiance was characterized by fitting the following model of photosynthesis with photoinhibition (Platt et al. 1980) for each sampling date:

$$P(I) = P_S(1 - e^{-\alpha I/P_S})e^{-\beta I/P_S}, \quad (6)$$

where  $P(I)$  is the productivity at irradiance  $I$ ,  $P_S$  is the potential productivity,  $\alpha$  is the slope of the light-saturation curve at low light levels, and  $\beta$  is the photoinhibition parameter. The maximum productivity  $P_{\max}$  was calculated as

$$P_{\max} = P_S \left( \frac{\alpha}{\alpha + \beta} \right) \left( \frac{\beta}{\alpha + \beta} \right)^{\beta/\alpha}. \quad (7)$$

Saturating irradiance for photosynthesis ( $I_k$ ) was calculated as  $P_{\max}/\alpha$ . A mean productivity irradiance curve was calculated using photosynthetic parameters, corresponding to the average of all the fitted photosynthetic parameters, throughout the summer (Table 2).

[19] To characterize the effect of internal waves on light climate, we estimated percent changes in

**Table 1** Physical, chemical, and biological parameters and date on which they were sampled.

Measured parameter	Sampling dates (in 2007)
Photosynthetically active radiation (PAR) and dissolved oxygen (DO) and fluorescence profiles	2, 15, 22 May
	12, 15, 26 June
	10, 24, 30 July
	1, 3, 6, 9, 21, 23, 28, 31 August
	7, 11, 18, 25 September
Phosphorus, nitrogen, and Chl <i>a</i> concentrations and gross photosynthetic oxygen production	2, 11 October
	30 July
	1, 3, 6, 9, 21, 23, 28, 31 August
	7, 11, 18, 25 September
	2, 11 October

productivity induced by the vertical displacements of the isotherm located at 5 m (DCM) compared with a constant 5-m depth, but not the lateral displacement, because the variability in the light climate along a horizontal plane likely is not as large. We characterized the vertical movement of the isotherm for each hour over a 2-week period (4–16 August 2007). The photosynthetic parameters were used to calculate the productivity for each hour, as well as observed values of surface  $I$  and  $K_d$  at 5 m (Table 2). We tested the hypothesis that the effects of internal waves on production are increased when seiche activity is in phase with high solar radiation, such that internal waves occur regularly during the daily cycle with a time period of a few hours. Change in productivity was averaged for each hour of the day and compared with the daily cycle in solar radiation and eastward surface current velocity (as a proxy of local wind forcing).

## Results

### Seasonal Thermal Structure

[20] Lake Bromont was thermally stratified throughout the summer, between May and September 2007 (Fig. 3A), with a thick metalimnion delimited by the bottom of the epilimnion down to the bottom of the metalimnion (Fig. 3B). The stratification intensity, measured by the Schmidt stability  $S_b$ , however, changed rapidly with high solar radiation associated with low wind forcing, gaining up to  $15 \text{ J m}^{-2} \text{ day}^{-1}$  on sunny days (Fig. 3A). The  $L_N$  fluctuated throughout the summer but was mostly between 1 and 12 (indicative of internal wave activity), remaining only temporarily (maximum 3 days in a row) above 12 (calm conditions) or below 1 (upwelling of hypolimnetic water) (Fig. 3C).

### Daily Physical Response to Wind Forcing and Internal Waves

[21] The responses of the thermal structure to short-term physical forcing are presented in Fig. 4 for the June focal period and Fig. 5 for the August focal period. Overall, the wind speed was greater during the August focal period than in June (Figs. 4A, 5A). The surface mixed layer deepened, resulting in a thinner metalimnion as summer progressed (Figs. 3B, 6A, B).

### June Focal Period

[22] Low wind speed, stable water column, shallow surface mixed layer (<2 m deep), and thick metalimnion (>4 m deep) characterized the physical structure of the water column in June. Wind had a diel periodicity, reaching a maximum between 10:00 h and 16:00 h, usually around noon (Fig. 4A). This 24-h periodicity can be seen in the spectral densities (Fig. 6A). Surface current velocity increased with the wind (Fig. 4A) and also had a diel periodicity indicated by the maximum spectral density at a period of 24 h (Fig. 6A). Surface current velocity increased in phase with the wind, except on 14 June, when low wind velocity was measured at Frelighsburg, while other meteorological stations in the region showed exceptional easterly wind reaching  $4 \text{ m s}^{-1}$ . Thermal structure changed significantly when surface current velocity exceeded  $10 \text{ cm s}^{-1}$ , which occurred three times during the focal period (Fig. 4A). Surface current velocities accurately highlighted wind events in the Lake Bromont area. Large temperature fluctuations were observed in the metalimnion with maximum amplitudes at 4.5 m depth (Fig. 4B).

[23] Two large wind events occurred on 16 and 17 June. Current velocity increased in phase with the wind,

**Table 2** Summary of the parameters used to compare the effect of seiches on light availability and photosynthetic activity. Light extinction coefficient, surface irradiance, and isotherm displacement ( $16^\circ\text{C}$  corresponding to the isotherm with the DCM) were similar to those observed during the period 4–16 August 2007.

Parameter	Mean $\pm$ SE	Units
Surface irradiance ( $I_0$ )	$756 \pm 838$	$\mu\text{mol photons m}^{-2} \text{ s}^{-1}$
Light extinction coefficient ( $K_d$ )	$0.8 \pm 0.1$	$\text{m}^{-1}$
Maximum productivity ( $P_S$ )	$6.36 \pm 3.10$	$\mu\text{g DO } \mu\text{g Chl } a^{-1} \text{ h}^{-1}$
Slope of light-saturation curve at low light levels ( $\alpha$ )	$0.34 \pm 0.09$	$\mu\text{g DO } \mu\text{g Chl } a^{-1} \text{ h}^{-1} (\mu\text{mol photons m}^{-2} \text{ s}^{-1})^{-1}$
Photoinhibition parameter ( $\beta$ )	$0.006 \pm 0.004$	$\mu\text{g DO } \mu\text{g Chl } a^{-1} \text{ h}^{-1} (\mu\text{mol photons m}^{-2} \text{ s}^{-1})^{-1}$

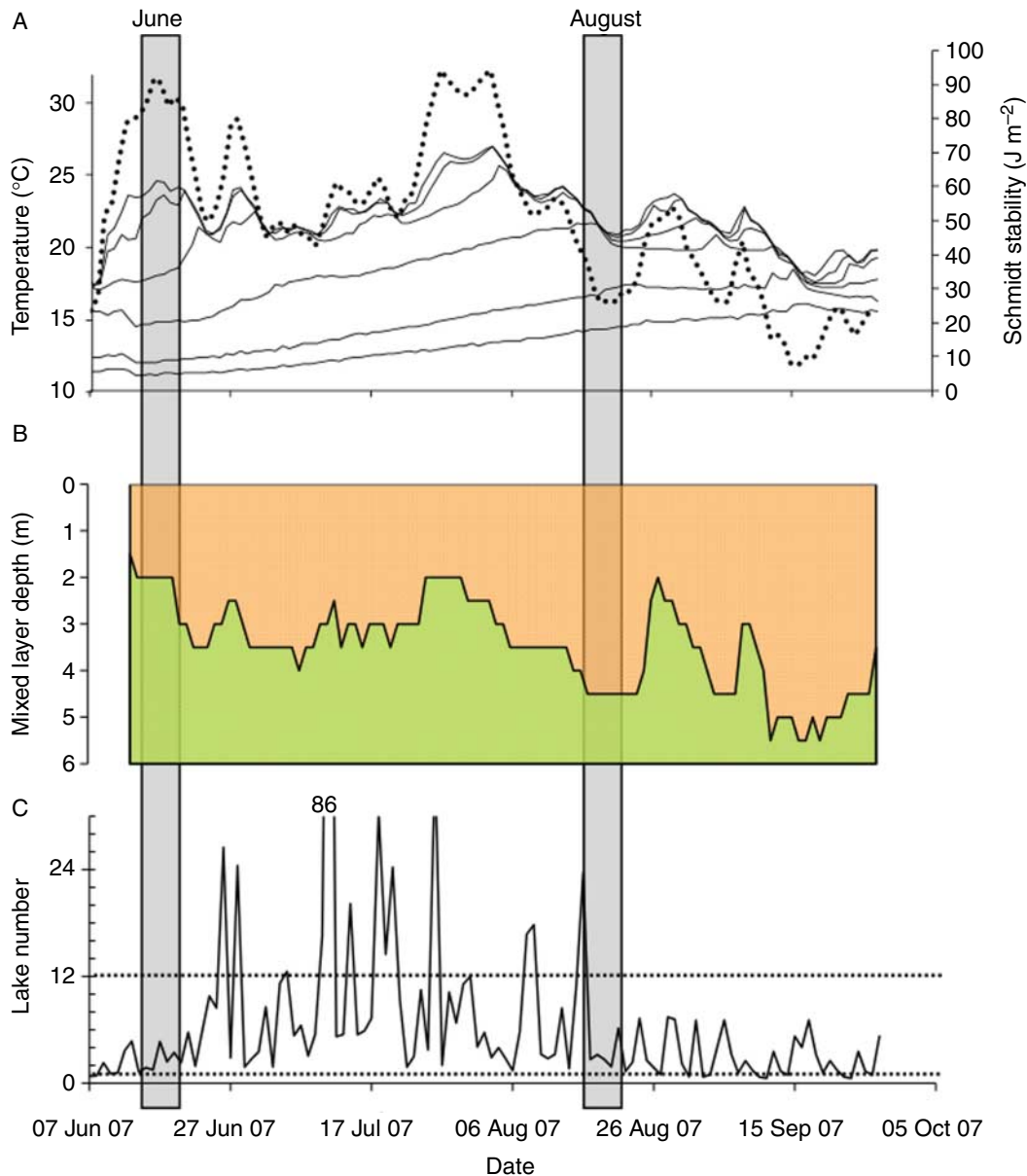


**Fig. 3** Summary of physical responses in Lake Bromont to wind forcing between June and September 2007, with shaded gray vertical lines showing the two focal periods: (A) mean daily water temperature (thin black lines) at different depths (1, 2, 3, 4, 5, and 5.5 m from the surface) and the Schmidt stability (dotted black line); (B) thickness of the epilimnion and the metalimnion delimited by the bottom of the epilimnion (uniform temperature); and (C) Lake number (the horizontal dotted line shows the threshold values of 1 and 12, between which internal waves can be observed). The maximum theoretical Lake number value is 86.

reaching a maximum speed of  $17.5 \text{ cm s}^{-1}$  (Fig. 4A). Large-amplitude and high-frequency temperature fluctuations were observed during the wind forcing events. The temperature within the metalimnion began to increase at 12:00 h and decreased after 14:00 h, with declining winds, followed by three complete oscillations

(Fig. 4A, B). These large temperature fluctuations with periodicity of about 3 h were in phase at different depths, indicating a first vertical mode seiche (Fig. 4C).

[24] Smaller amplitude temperature fluctuations ( $< 1^\circ \text{C}$ ) dominated in the metalimnion between periods of wind forcing, with fluctuations as high as

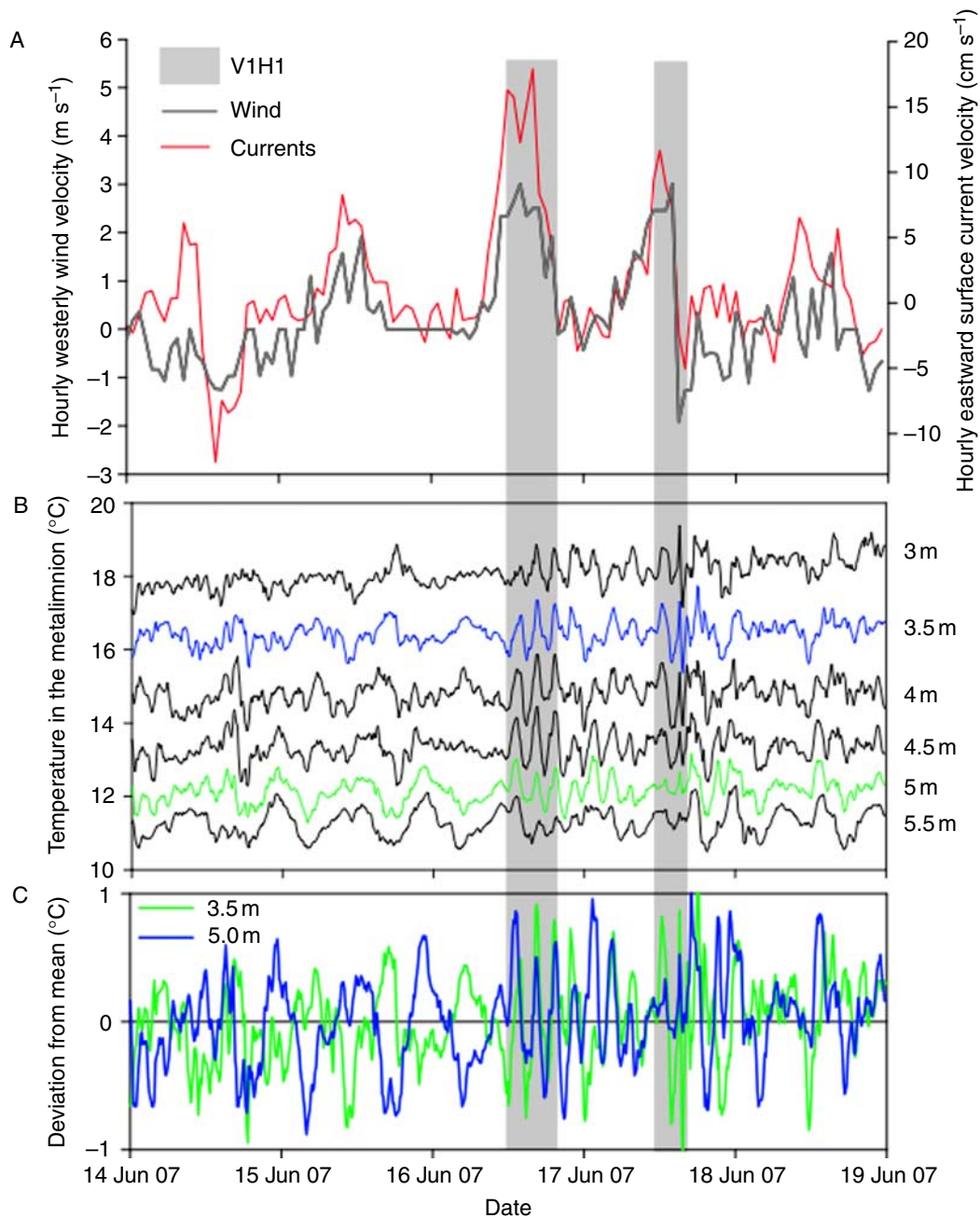


**Fig. 4** Detailed physical observations from the June focal period (from 14 June 0:00 h to 19 June 0:00 h): (A) hourly westerly wind speed during the 5-day period (gray line) and hourly eastward surface current velocity (red line); (B) temperature series measured by the thermistor chain at 3, 3.5, 4, 4.5, 5, and 5.5 m depths; and (C) temperature deviations from daily means at depths of 5.0 and 3.5 m. Gray areas represent examples of periods during which V1H1 dominated.

2°C at 5.5 m (Fig. 4B). Temperature fluctuations were out of phase at 3.5 and 5 m (Fig. 4C), corresponding to a higher vertical mode predominating between periods of first vertical mode dominance.

[25] Periods of first, second, and third vertical mode seiches were calculated as 4.1 h, 7.4 h, and 10.7 h, respectively (Table 3), for the real bathymetry. Peak spectral density calculated from temperature at

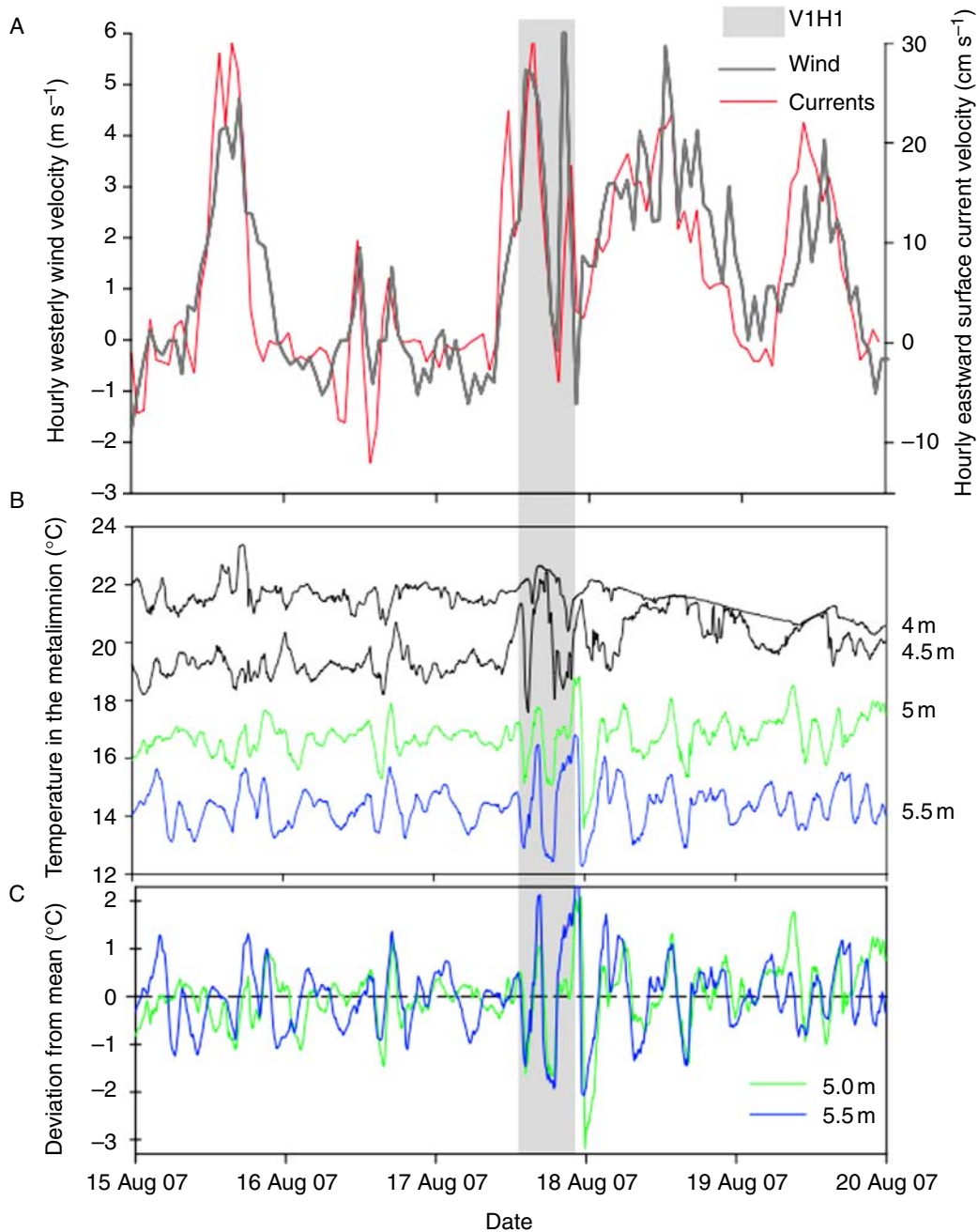


**Fig. 5** Detailed physical observations from the August focal period (from 15 August 0:00 h to 20 August 0:00 h): (A) hourly westerly wind speed during the 5-day period (gray line) and hourly eastward surface current velocity (red line); (B) temperature series measured by the thermistor chain at 4, 4.5, 5, and 5.5 m depths; and (C) temperature deviations from daily means at depths of 5.5 and 5.0 m. Gray areas represent examples of periods during which V1H1 dominated.

the different depths indicated three periodicities: 3.1 h between 3.5 and 4.5 m, 7.5 h between 3.5 and 5.5 m, and 12 h between 2.5 and 5.5 m (Fig. 6E), with each period corresponding to the occurrence of each of the predicted

vertical mode seiches, and the highest amplitude associated with the V3H1. The model with real bathymetry gave calculated periods very close to observed values (Fig. 6E and Table 3). In summary, first, second, and

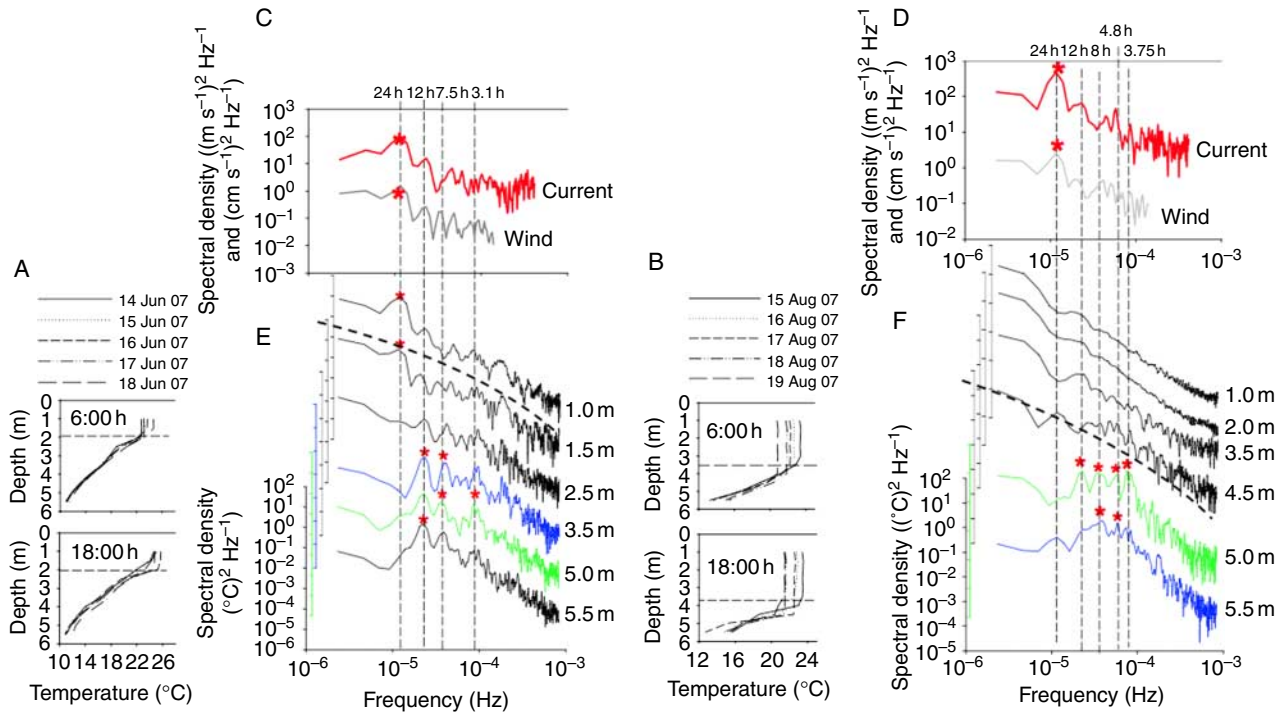


**Fig. 6** (A and B) Depth profiles of temperature for each day at 06:00 h and 18:00 h, with a horizontal dotted line showing the start of the metalimnion, for the 5-day period (A) in June 2007 and (B) in August 2007; (C and D) power spectral density for wind speed (gray line) and current velocity (red line), for the 5-day period (C) in June and (D) in August; and (E and F) power spectral density for the temperature time series between 1 m and 5.5 m (staggered by depth), (E) in June and (F) in August. Vertical black dotted lines represent periods of fluctuations and asterisks show dominant periods.

third vertical mode seiches were observed, with V1H1 mode just after wind relaxation, after which both V2H1 and V3H1 modes dominated.

#### August Focal Period

[26] High wind speed, a deep surface mixed layer (about 4 m), and a thin metalimnion characterized the August focal period. The surface mixed layer was initially 3.5 m deep on 15 August, increasing to 4.5 m by 17 August (Fig. 6B). Wind forcing in August was stronger than in June, leading to higher current velocity (Fig. 5A). The daily periodicity of both wind speed and surface current velocity was evident in the peak spectral density (Fig. 6D). Owing to the continuous decrease of temperature in the epilimnion and the decreasing stability of the water column in August, no periodicity in temperature fluctuations could be identified in the epilimnion, as had been seen in June when daily cycles of warming and cooling were observed in surface waters (Fig. 6F).

[27] Large fluctuations of temperature (up to 3°C) in the metalimnion alternated with smaller ones (up to 1°C) and occurred in parallel with wind forcing (Fig. 5B). Smaller fluctuations were sometimes in phase and sometimes out of phase (Fig. 5C). Periods of about 5 h with large temperature fluctuations in phase

**Table 3** Calculated and observed periods of the various seiche modes for the metalimnion temperature time series, in June and August 2007.

Focal period	Analytical solution (h)	Real bathymetry (h)	Observed periods (h)
14–18 June			
V1H1	5.2	4.1	3.1
V2H1	10.4	7.4	7.5
V3H1	15.7	10.7	12
15–19 August			
V1H1	4.2	4.8*	3.75 and 4.8
V2H1	8.3	7	8
V3H1	12.5	9.1	12

\* Calculated with a grid resolution of  $31 \times 31$  (instead of  $41 \times 41$ ).

throughout the water column (V1H1) were observed, as on 15 and 17 August (Fig. 5).

[28] The calculated periodicity of V1H1, V2H1, and V3H1 modes, for the real bathymetry, were 4.8 h, 7.0 h, and 9.1 h, respectively (Table 3). Power spectral densities of temperature were greatest for 3.75 h at 5 m, corresponding to the frequency of the V1H1 mode (Fig. 6E, F). Two other peaks at 8 h and 12 h corresponded to the frequency of V2H1 and V3H1 (Fig. 6F). These periods are close to the analytical solutions (Table 3) and highlight the occurrence of at least the three first types of vertical modes during August. Strong physical forcing induced a deepening of the mixed layer depth and a reduction in water column stability, while first, second, and third vertical mode seiches were observed.

[29] During both focal periods, fluctuations of temperature at depth varied in amplitude and phase as a result of V1H1, V2H1, and V3H1 modes, generated by wind forcing. The V1H1 mode was rapidly dissipated, while V2H1 and V3H1 oscillations dominated the rest of the time.

#### *Amplitude of Vertical Movement*

[30] The movement of metalimnetic layers with wind forcing is evident from the temperature fluctuations (Figs. 4C, 5C). In-phase oscillations at different depths (V1H1) alternated with out-of-phase oscillations that increased and decreased the thickness of the metalimnetic layer (Figs. 4B, C; 5B, C). The vertical displacement of isotherms, which depends on the three modes, showed the highest peak-to-peak amplitude, with 80 cm in June and 60 cm in August. A complete absence of metalimnetic temperature fluctuations was never observed in the summer of 2007, indicating persistent internal wave activity.

#### *Light Climate and Productivity*

[31] Saturating irradiance ( $I_k$ ) was  $35 \mu\text{mol photons m}^{-2} \text{s}^{-1}$  (Fig. 7A). This was observed at depths larger than 4.5 m until early August (Fig. 7B). Metalimnetic productivity at 5 m remained significant until mid-August. There was only a small increase when communities were incubated at mid-depth (Fig. 7B), suggesting that the light climate was close to optimum at the DCM.

This is consistent with the persistence of a productive metalimnetic layer and relatively high DO (up to  $12 \text{ mg L}^{-1}$ ) observed from July to 5 August 2007 (Fig. 8B). DCM productivity was close to zero after mid-August, but it was high when communities were brought to the surface (Fig. 7B). Mid-depth incubated communities decreased in productivity as summer progressed, finally reaching zero in mid-September (Fig. 7B). These productivity changes indicate light limitation at 5 m depth and a tendency for limitation to move upward later in the season (Fig. 7C).

#### *Phosphorus and Nitrogen Availability*

[32] Nutrient inputs from rivers entering Lake Bromont remained low throughout the summer (McMeekin 2009). Strong vertical gradients in P and N concentrations were observed in the stratified period (Fig. 8C, D), linked to a bottom anoxic layer, observed all summer (Fig. 8B). TDP remained  $< 5 \mu\text{g PL}^{-1}$  to a depth of 5 m until the beginning of September and increased with depth up to  $100 \mu\text{g PL}^{-1}$  (Fig. 8C). Similarly, TDN was on average  $205 \mu\text{g NL}^{-1}$  between the surface and 5 m and as high as  $1400 \mu\text{g NL}^{-1}$  at 5.5 m depth (Fig. 8D). Based on these gradients, vertical fluxes of dissolved nutrients between 5.5 and 6 m were inferred both using low vertical diffusivity  $K_z$  ( $1.4 \times 10^{-7} \text{ m}^2 \text{ s}^{-1}$ ), as  $0.8 \pm 0.3 \mu\text{g PL}^{-1} \text{ day}^{-1}$  and  $14.2 \pm 3.7 \mu\text{g NL}^{-1} \text{ day}^{-1}$ , and using typical  $K_z$  associated with seicheing ( $2 \times 10^{-5} \text{ m}^2 \text{ s}^{-1}$ ), as  $112 \pm 46 \mu\text{g PL}^{-1} \text{ day}^{-1}$  and  $2030 \pm 530 \mu\text{g NL}^{-1} \text{ day}^{-1}$ .

#### *Biological Structure*

[33] From June to mid-August, the phytoplankton community was dominated by metalimnetic populations located at 5 m depth, indicated by Chl *a* fluorescence just above the anoxic layer (Fig. 8A, B). In mid-August, deepening of the surface mixed layer induced entrainment of biomass into the epilimnion (Fig. 8A). In mid-September, following the autumn overturn, the phytoplankton vertical distribution changed from metalimnetic to epilimnetic domination (Fig. 8A) and was associated with a decline in the Schmidt stability number (Fig. 3A) and with a lake number  $L_N$  value  $< 1$  (Fig. 3C).

*Ecological Consequences of Seiche Activity for Metalimnetic Communities: Depth-Related Frequency of Temperature Fluctuations*

[34] Epilimnetic water showed daily changes in temperature associated with daytime warming and nighttime cooling, while metalimnetic waters showed temperature fluctuations on shorter time scales (Fig. 6E, F). The maximum amplitudes of the spectral densities in the metalimnion, in particular at 5 and 5.5 m, were similar to those in the epilimnion, although with shorter

periods varying between 3 and 12 h, which were observed in both June and August (Fig. 6E, F). These fluctuations were associated with internal wave activity. The shortest period corresponded to VIH1 and was located at the depth of the DCM. In June, the minimum period of 3.1 h was located at 4.5 m (Fig. 6E), while the minimum period of 3.75 h was at 5 m during the August focal period (Fig. 6F). Consequently, a vertical gradient of temperature fluctuation frequency was observed, in addition to the opposing gradients of light and nutrients.

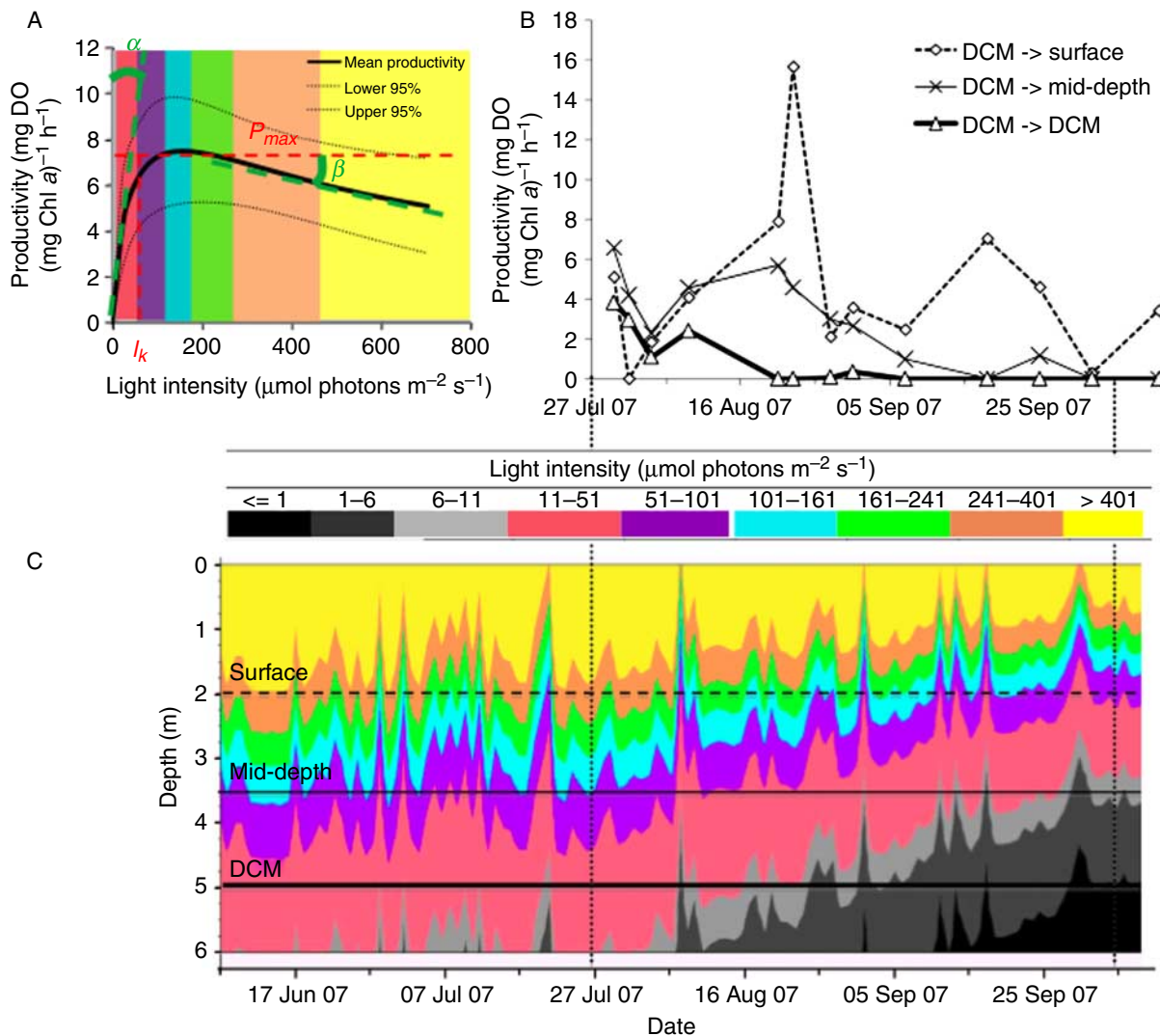


**Fig. 7** (A) Mean productivity irradiance curve with its confidence interval (calculated from photosynthetic parameters averaged over all the fitted photosynthetic parameters, throughout the summer; see Table 2) of the metalimnetic community (at 5 m depth). The four photosynthetic parameters (see Table 2) are shown. (B) Productivity (averaged between 10:00 h and 15:00 h) of the metalimnetic community (DCM) incubated in situ at 2 m depth ("surface"), at 3.5 m depth ("mid-depth"), and at 5 m depth (initial depth; "DCM"). (C) Evolution of PAR irradiance by depth averaged daily between 10 and 15 h (corresponding to the time period of productivity measurements). The quantitative color scheme of A is maintained in C. Horizontal lines show incubation depths of B.

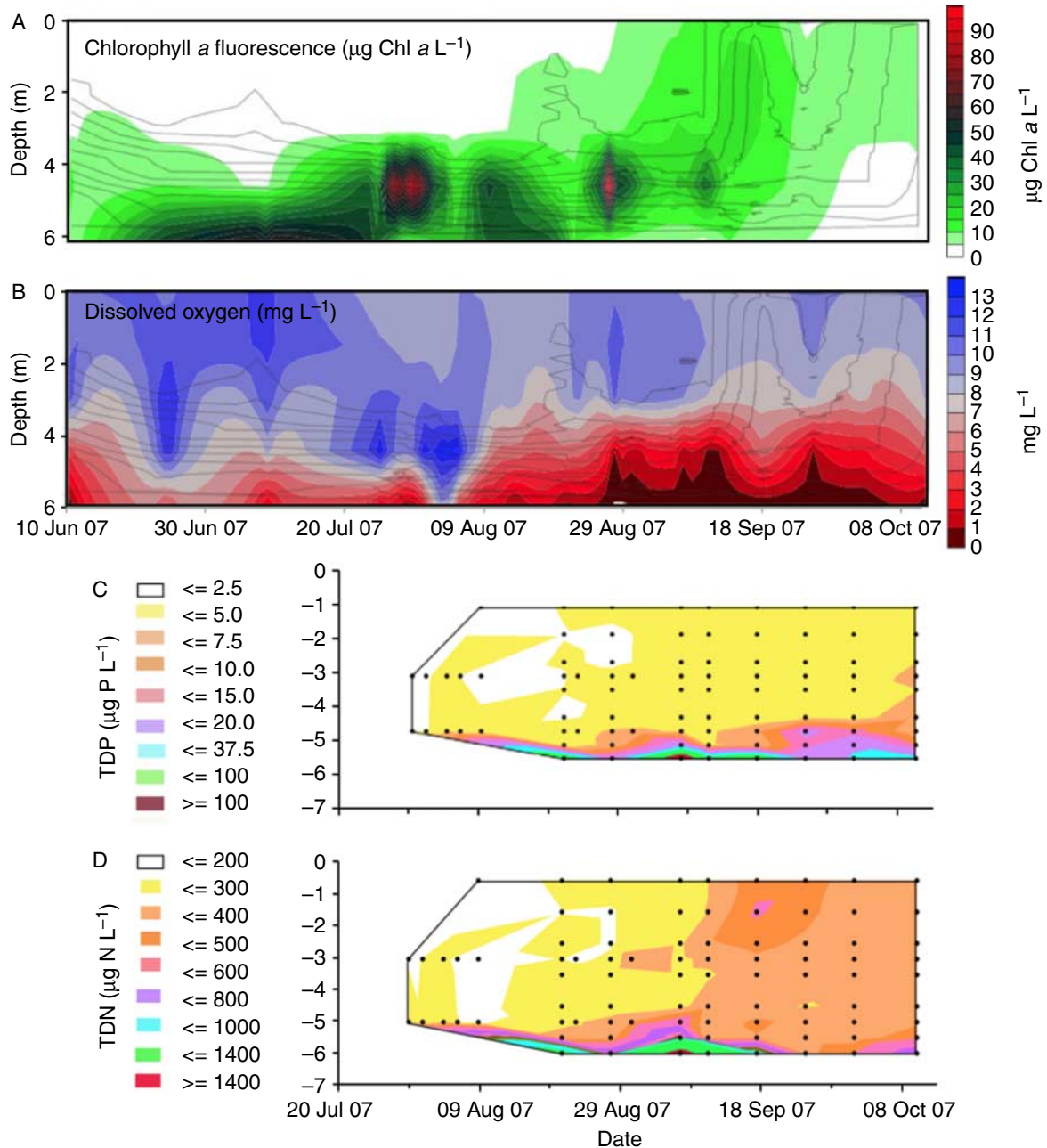


**Fig. 8** Time series of vertical profiles of (A) fluorescence (estimate of total Chl *a* biomass,  $\mu\text{g L}^{-1}$ ), (B) dissolved oxygen ( $\text{mg DO L}^{-1}$ ), (C) total dissolved phosphorus (TDP;  $\mu\text{g P L}^{-1}$ ), and (D) total dissolved nitrogen (TDN;  $\mu\text{g N L}^{-1}$ ), over the entire sampling season (June to September 2007). The black lines in A and B represent the isotherms.

#### Light Availability and Internal Waves

[35] We characterized the effects of vertical displacement of phytoplankton cells induced by internal waves through the light gradient, to determine how internal waves might be affecting photosynthetic activity. During

the June period, 2.4% of incident light reached 5 m depth, and given the observed vertical displacement of 80 cm, light varied between 25.2 and 46.2  $\mu\text{mol photons m}^{-2} \text{s}^{-1}$ . Such variation in light climate induced a productivity change between  $-20\%$  and  $+25\%$ , compared

with constant light. During the August focal period, light varied between 6.0 and 10.8  $\mu\text{mol photons m}^{-2}\text{s}^{-1}$ , and thus productivity was between  $-27\%$  and  $+26\%$ , given the observed isotherm displacement of 60 cm. The effects of internal waves can increase when upward movements occur in phase with solar radiation. To test this effect, we calculated the mean percentage of change in photosynthetic activities with time of day (Fig. 9). Productivity with internal waves was up to 9% higher between 9:30 h and 14:30 h, and up to 5% lower between 15:30 h and 18:30 h, compared with no internal waves (Fig. 9).

### Discussion

[36] Lake Bromont represents one of the smallest and shallowest lentic ecosystems for which recurrent internal waves have been described. A strong vertical temperature gradient over the summer, often higher than  $10^\circ\text{C}$  between the surface and the bottom, increased water column stability. However, although the lake is surrounded by forests and hills, it is exposed along an

east-west axis, which most likely led to a funnel effect of the dominant winds. Wind speed and its periodicity, lake morphometry, and the general shape of the thermal structure are the main factors that explain the presence and modes of internal waves in lakes (LaZerte 1980; Wiegand and Chamberlain 1987). In this study, wind was subject to diurnal variation with maximum speed recorded between 10:00 and 16:00 h, strongly influencing the lake temperature and current distribution, particularly near the surface (Fig. 9). A strong correlation was observed between wind speed and surface current, with a time lag shorter than 1 h.

[37] Although the two focal periods differed in terms of water column stability and wind forcing, the internal wave responses were similar, with the occurrence of the first, second, and third vertical modes at subdiurnal frequencies. The second and third vertical mode seiches dominated in time over the first mode. V1H1 was initiated for only a few hours during large westerly wind events and when the Lake number ( $L_N$ ) decreased to approximately 1, as also observed by Vidal et al. (2007). Higher modes dominated when  $L_N$  was between 1 and 12, when the restoring force was larger than the forces perturbing the system and the tilting of the isotherms was small compared to the thickness of the epilimnion (Vidal et al. 2007). Because dissipation time scales with wave period (Fischer et al. 1979), one would expect first vertical mode seiches (V1H1) with shorter periods to be rapidly dampened, and higher vertical modes to persist for longer periods, as we observed. In small lakes, a higher dissipation of internal wave energy on the boundaries can be expected due to a larger proportion of the BBL over larger lakes, which would result in rapid dampening of all internal waves. The persistence of the higher modes, however, can be explained by the resonance of the waves (in particular, V3H1, with a period of 12 h) with the same subperiodicity as the wind. Similar behavior has been described by Vidal et al. (2007) and Wiegand and Chamberlain (1987). In particular, when the metalimnion is thick relative to the depth of the water column, higher vertical modes can be excited by wind with a regular periodicity (Münnich et al. 1992). Higher vertical modes also displayed larger peaks on the power spectral density (in June) compared with the first mode, indicating a higher

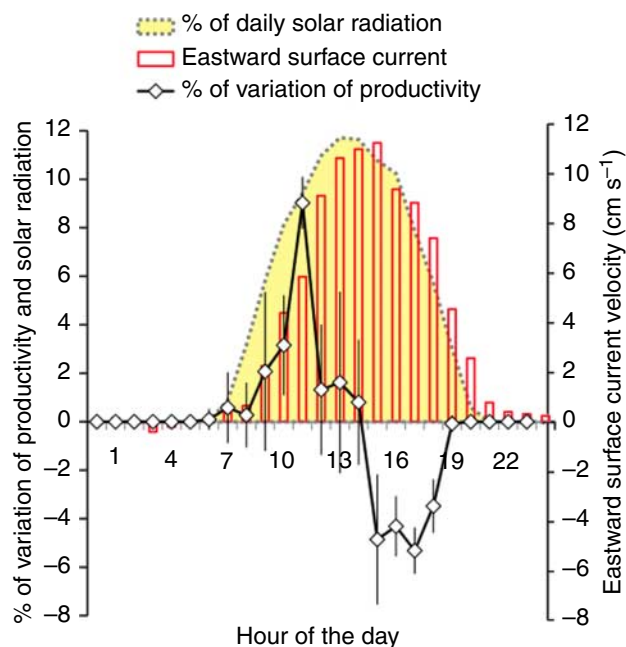


**Fig. 9** Gain of hourly averages of productivity in the presence of internal waves (based on isotherm displacement) compared with an absence of internal waves (constant depth), calculated between 4 and 16 August 2007. Hourly mean eastward current velocity (histogram) and percentage of daily surface light intensity (yellow area) are also shown.

amplitude of these modes, induced by the resonance with daily wind at that time, as observed previously (Münnich et al. 1992). Internal waves were observed in our lake throughout the summer, indicating that daily winds were sufficient to sustain them with consequences for the ecological functioning of the lake.

[38] Persistent thermal stratification led to an anoxic layer and strong vertical gradients of nutrients. Nutrients were thus supplied to the epilimnion through vertical turbulent diffusion associated with internal waves, and possibly through horizontal redistribution as suggested by MacIntyre et al. (1999). Light, which attenuates rapidly with depth, reached limiting values at the base of the metalimnion. The two essential resources for phytoplankton communities, light and nutrients, were thus vertically separated, structuring the vertical distribution of phytoplankton biomass in accordance with other studies (Huisman and Weissing 1995; Diehl 2002). Phytoplankton communities formed a thin layer, a DCM, at the optimal depth in terms of light and nutrient, as per the “algal game” (Klausmeier and Litchman 2001). The vertical location of metalimnetic peaks, resulting from a trade-off between light and nutrients, depends on the relative competitive abilities for each resource type of the phytoplankton species present. Good competitors for light tend to move downward, while good competitors for nutrients tend to move upward (Klausmeier and Litchman 2001).

[39] Cyanobacteria, particularly *Planktothrix agardhii* and several species of *Aphanizomenon*, dominated Lake Bromont’s metalimnetic communities all summer (Pannard et al., pers. comm.). These cyanobacteria taxa have lower light requirements than most because they contain phycobilins, but they are not considered good competitors for nutrients because they are sensitive to P limitation (Reynolds et al. 2002). In the epilimnion, TDP was low ( $2.29 \pm 0.70 \mu\text{g PL}^{-1}$ ) and nitrate concentration remained close to zero, suggesting that P (and perhaps also N) must have limited growth. In June, the maximum phytoplankton biomass was located in the bottom part of the thick metalimnion. This was despite light limitation as demonstrated by the increase in productivity that occurred when this metalimnetic community was incubated at shallower depths. The strong accumulation of phytoplankton biomass at

the bottom of the 4-m-thick metalimnion suggests that this community was dominated by good-light but poor-nutrient competitors (Klausmeier and Litchman 2001).

[40] Metalimnetic populations were exposed to internal waves and to their recurrent oscillating movements. We observed several ecological effects and advantages of such internal waves for phytoplankton production. The deeper vertical fluxes of N and P (between 5.5 and 6 m) associated only with low vertical diffusivity were not sufficient to explain the high biomass of phytoplankton in the metalimnion. This demonstrates indirectly the necessity of turbulent mixing. While a flux of  $1 \mu\text{g PL}^{-1} \text{day}^{-1}$  corresponds to a maximum of  $0.83 \mu\text{g Chl } a \text{ L}^{-1} \text{day}^{-1}$  according to stoichiometric ratios (Reynolds 2006), we observed a biomass metalimnetic peak that was more than 30 times higher. Internal waves can also generate mixing and upward nutrient fluxes at sloping boundaries, leading to horizontal intrusions of water into the pelagic zone and vertical nutrient supply to the phytoplankton DCM (MacIntyre and Jellison 2001). For example, in Mono Lake (California), BBL transport increased upward ammonium fluxes by 53%, resulting in a 6% increase in photic zone primary production (Bruce et al. 2008). Because the largest part of internal wave energy is dissipated at lake boundaries (Münnich et al. 1992), a strong dissipation of energy is expected in small lakes, leading to enhanced vertical transport of nutrients, whereas the small size minimizes horizontal differences between littoral and pelagic areas. The relatively large BBL in small lakes should increase the effect of nutrient fluxes on overall productivity, mainly in the epilimnion for eutrophic lakes and the metalimnion for oligomesotrophic lakes.

[41] Vertical displacements associated with internal wave activity induce variability in light availability, which we found benefits primary production. In our study, productivity was measured using in situ incubations lasting 5 h (between 10:00 h and 15:00 h), so as to partially integrate diel variation in photosynthetic parameters. In this way we captured the greatest diel variation in parameters, which was also observed in two lakes geographically close to ours (Forget et al. 2009), where only a 10% increase at noon over morning sampling (6:00 h) was detected. Our results demonstrate

that metalimnetic photosynthetic productivity fluctuated up to  $\pm 20\%$ – $25\%$  around the nonseiching mean value, because of internal waves, and that the effect was highest when solar radiation and internal wave oscillations were in phase. This periodically changing light environment can influence the coexistence of phytoplankton species through niche separation and species competition mediation (Flöder et al. 2002). Walsh and Legendre (1983) showed that under fluctuating light induced by sea surface waves ( $\pm 50\%$  of constant light levels), maximum productivity remained the same, but photosynthetic efficiency was increased by 30%. Evans et al. (2008) demonstrated that the photosynthetic rates of phytoplankton circulated at depths mimicking isotherm displacement in a light-limited field were higher than those of phytoplankton incubated in static incubations. Based on the application of this model to our study, we found that internal waves increased primary production of metalimnetic communities in Lake Bromont.

[42] The phytoplankton community in our study was exposed to multiple vertical environmental gradients due to internal waves, specifically opposing overall gradients in light and nutrient resources and fluctuating gradients of environmental changes, associated with both vertical and horizontal displacements in surface waters at the daily scale and at the scale of a few hours in deeper waters. Temperature variability induced by internal waves can increase diversity of benthic microalgal communities when comparing upwind and downwind communities (McCabe and Cyr 2006). Similar results are expected along the vertical gradient of environmental conditions in lakes exposed to internal waves. The high frequency of changes in physical and chemical conditions, from  $6 \text{ day}^{-1}$  to  $2 \text{ day}^{-1}$ , can influence phytoplankton physiology and production. Even if the community structure changes at time scales longer than a day (Hyenstrand et al. 2000; Yamamoto and Hatta 2004), nutrient uptake rates and changes in cell nutrient quotas fluctuate at higher frequencies. One can thus hypothesize that species with low storage capacity but high growth rates gain a competitive advantage over storage strategists in the presence of recurrent internal waves. This is particularly relevant for a metalimnetic

community, typically known to consist of species that are poor competitors for nutrients, as discussed above.

[43] The vertical excursion of the metalimnion induced by seiches, together with its mixing characteristics, influenced both light and nutrient availability for the phytoplankton community and overall photosynthetic activity. Seiche activity increases temporal variability of the physical and chemical conditions along the vertical gradient. It has been previously demonstrated that different time scales in physical and chemical forcing induce different responses in the phytoplankton community, in terms of diversity, rate of community change, and dominant and indicator species (Pannard et al. 2008). To further link the physical and biological response of a metalimnetic phytoplankton community to wind forcing, fine scale sampling of the metalimnetic phytoplankton is needed, in particular an hourly survey of its activity (to test for physiological adaptations) and a daily survey of the community structure (to test for biological interactions, e.g., competition).

#### *Significance to Aquatic Environments*

[44] Despite the numerical dominance of small versus large lakes, the influence of short-term physical forcing has largely been neglected in ecological investigations of such ecosystems. This study examined the physical and biological responses to wind forcing in a small stratified lake, by characterizing the frequency and amplitude of internal waves and examining the ecological implications for metalimnetic phytoplankton productivity. We found that large populations of phytoplankton may accumulate in the metalimnion, being at the interface of deeper nutrient-rich water and shallower illuminated water, thereby leading to a DCM. Internal waves, which enhance vertical nutrient fluxes, also induce vertical excursion of these metalimnetic populations in the light-limited field, which may increase photosynthetic activity and biomass, if the fluctuations are in phase. The productivity of small stratified lakes therefore depends on wind disturbance, which can resuspend algal cells and enhance upward fluxes of nutrients.

*Acknowledgments* We thank S. Paquet, C. Beauchemin, P. Marcoux, K. McMeekin, and M. Jourdain for field and laboratory assistance and for the bathymetry of the lake (S. Paquet). We are grateful to

Yvan Lagadeuc for valuable discussion and comments. We thank J. D. Ackerman, S. Monismith, and three anonymous referees for helpful comments on an earlier version of the manuscript. This research was funded by a grant from the Fonds Québécois de la Recherche sur la Nature et les Technologies to D. F. B., B. E. B., and D. P. and by the Groupe de Recherche Interuniversitaire en Limnologie. We thank the Action de conservation du bassin versant du lac Bromont for the bathymetric map, for the infrastructure support, and for logistical help in the field.

## References

- Beisner, B. E. 2001. Plankton community structure in fluctuating environments and the role of productivity. *Oikos*. **95**: 496–510, doi:10.1034/j.1600-0706.2001.950315.x.
- Bormans, M., P. W. Ford, L. Fabbro, and G. Hancock. 2004. Onset and persistence of cyanobacterial blooms in a large impounded tropical river, Australia. *Mar. Freshwater Res.* **55**: 1–15, doi:10.1071/MF03045.
- Bruce, L., R. Jellison, J. Imberger, and J. Melack. 2008. Effect of benthic boundary layer transport on the productivity of Mono Lake, California. *Saline Systems*. **4**: 11, doi:10.1186/1746-1448-4-11.
- Carignan, R., A.-M. Blais, and C. Vis. 1998. Measurement of primary production and community respiration in oligotrophic lakes using the Winkler method. *Can. J. Fish. Aquat. Sci.* **55**: 1078–1084, doi:10.1139/cjfas-55-5-1078.
- Carignan, R., D. Planas, and C. Vis. 2000. Planktonic production and respiration in oligotrophic Shield lakes. *Limnol. Oceanogr.* **45**: 189–199, doi:10.4319/lo.2000.45.1.0189.
- Carrick, H., F. Aldridge, and C. Schelske. 1993. Wind influences phytoplankton biomass and composition in a shallow, productive lake. *Limnol. Oceanogr.* **38**: 1179–1192, doi:10.4319/lo.1993.38.6.1179.
- Cattaneo, A., and Y. T. Prairie. 1995. Temporal variability in the chemical characteristics along the Rivière de l'Assiniboia: How many samples are necessary to describe stream chemistry. *Can. J. Fish. Aquat. Sci.* **52**: 828–835, doi:10.1139/f95-082.
- Cozar, A., J. A. Galvez, V. Hull, C. M. Garcia, and S. A. Loiselle. 2005. Sediment resuspension by wind in a shallow lake of Esteros del Ibera (Argentina): A model based on turbidimetry. *Ecol. Model.* **186**: 63, doi:10.1016/j.ecolmodel.2005.01.020.
- Diehl, S. 2002. Phytoplankton, light and nutrients in a gradient of mixing depths: Theory. *Ecology*. **83**: 386–398, doi:10.1890/0012-9658(2002)083[0386:PLANIA]2.0.CO;2.
- Downing, J. A., et al. 2006. The global abundance and size distribution of lakes, ponds, and impoundments. *Limnol. Oceanogr.* **51**: 2388–2397, doi:10.4319/lo.2006.51.5.2388.
- Environment Canada. 2007. Rapport de données horaires pour le 01 juin, 2007. [http://climate.weatheroffice.gc.ca/climate\\_data/hourlydata\\_f.html?timeframe=1&Prov=XX&StationID=31829&Month=6&Day=1&Year=2007&cmdB1=Allez](http://climate.weatheroffice.gc.ca/climate_data/hourlydata_f.html?timeframe=1&Prov=XX&StationID=31829&Month=6&Day=1&Year=2007&cmdB1=Allez).
- Evans, M. A., S. MacIntyre, and G. W. Kling. 2008. Internal wave effects on photosynthesis: Experiments, theory, and modeling. *Limnol. Oceanogr.* **53**: 339–353, doi:10.4319/lo.2008.53.1.0339.
- Fischer, H. B., E. J. List, R. C. Y. Koh, J. Imberger, and N. H. Brooks. 1979. *Mixing in Inland and Coastal Waters*. Academic Press.
- Flöder, S., J. Urabe, and Z.-i. Kawabata. 2002. The influence of fluctuating light intensities on species composition and diversity of natural phytoplankton communities. *Oecologia*. **133**: 395–401, doi:10.1007/s00442-002-1048-8.
- Forget, M.-H., R. Carignan, and C. Hudon. 2009. Influence of diel cycles of respiration, chlorophyll, and photosynthetic parameters on the summer metabolic balance of temperate lakes and rivers. *Can. J. Fish. Aquat. Sci.* **66**: 1048–1058, doi:10.1139/F09-058.
- Fricker, P. D., and M. H. Nepf. 2000. Bathymetry, stratification, and internal seiche structure. *J. Geophys. Res.* **105**: 14237–14251.
- Håkanson, L., and M. Lindstrom. 1997. Frequency distributions and transformations of lake variables, catchment area and morphometric parameters in predictive regression models for small glacial lakes. *Ecol. Model.* **99**: 171–201, doi:10.1016/S0304-3800(97)01951-0.
- Hanson, P., S. Carpenter, J. Cardille, M. Coe, and L. Winslow. 2007. Small lakes dominate a random sample of regional lake characteristics. *Freshwater Biol.* **52**: 814–822, doi:10.1111/j.1365-2427.2007.01730.x.
- Heinz, G., J. Imberger, and M. Schimmele. 1990. Vertical mixing in Überlinger See, western part of Lake Constance. *Aquat. Sci.* **52**: 256–268, doi:10.1007/BF00877283.
- Huisman, J., and F. J. Weissing. 1995. Competition for nutrients and light among phytoplankton species in a mixed water column: theoretical studies. *Water Sci. Tech.* **32**: 143–147, doi:10.1016/0273-1223(95)00691-5.
- Hyenstrand, P., U. Burkert, A. Pettersson, and P. Blomqvist. 2000. Competition between the green alga *Scenedesmus* and the cyanobacterium *Synechococcus* under different modes of inorganic nitrogen supply. *Hydrobiologia*. **435**: 91–98, doi:10.1023/A:1004008721373.
- Imberger, J. 1998. Flux paths in a stratified lake: A review. Pp. 1–17. *In* J. Imberger [ed.], *Physical Processes in Lakes and Oceans*. Coast. Estuarine Stud. American Geophysical Union.
- Imberger, J., and G. Parker. 1985. Mixed layer dynamics in a lake exposed to a spatially variable wind field. *Limnol. Oceanogr.* **30**: 473–488, doi:10.4319/lo.1985.30.3.0473.
- Imberger, J., and J. C. Patterson. 1989. Physical limnology. *Adv. Appl. Mech.* **27**: 303–475, doi:10.1016/S0065-2156(08)70199-6.
- Jöhnk, K. D., J. Huisman, J. Sharples, B. Sommeijer, P. M. Visser, and J. M. Stroom. 2008. Summer heatwaves promote blooms of harmful cyanobacteria. *Glob. Change Biol.* **14**: 495–512, doi:10.1111/j.1365-2486.2007.01510.x.
- Klausmeier, C. A., and E. Litchman. 2001. Algal games: The vertical distribution of phytoplankton in poorly mixed water columns.

- Limnol. Oceanogr. **46**: 1998–2007, doi:10.4319/lo.2001.46.8.1998.
- LaZerte, B. D. 1980. The dominating higher order vertical modes of the internal seiche in a small lake. *Limnol. Oceanogr.* **25**: 846–854, doi:10.4319/lo.1980.25.5.0846.
- MacIntyre, S., K. M. Flynn, R. Jellison, and J. R. Romero. 1999. Boundary mixing and nutrient fluxes in Mono Lake, California. *Limnol. Oceanogr.* **44**: 512–529, doi:10.4319/lo.1999.44.3.0512.
- MacIntyre, S., and R. Jellison. 2001. Nutrient fluxes from upwelling and enhanced turbulence at the top of the pycnocline in Mono Lake, California. *Hydrobiologia.* **466**: 13–29, doi:10.1023/A:1014563914112.
- MacIntyre, S., J. O. Sickman, S. A. Goldthwait, and G. W. Kling. 2006. Physical pathways of nutrient supply in a small, ultraoligotrophic arctic lake during summer stratification. *Limnol. Oceanogr.* **51**: 1107–1124, doi:10.4319/lo.2006.51.2.1107.
- McCabe, S. K., and H. Cyr. 2006. Environmental variability influences the structure of benthic algal communities in an oligotrophic lake. *Oikos.* **115**: 197–206, doi:10.1111/j.2006.0030-1299.14939.x.
- McMeekin, K. 2009. Le bilan de phosphore du Lac Bromont: Vers l'identification des activités humaines causant les blooms de cyanobactéries, MSc thesis, Université du Québec à Montréal.
- Mortimer, C. H. 1953. The resonant response of stratified lakes to wind. *Aquat. Sci.* **15**: 94–151.
- Münnich, M., A. Wüest, and D. M. Imboden. 1992. Observations of the second vertical mode of the internal seiche in an alpine lake. *Limnol. Oceanogr.* **37**: 1705–1719, doi:10.4319/lo.1992.37.8.1705.
- Ostrovsky, I., Y. Z. Yacobi, P. Walline, and I. Kalikhman. 1996. Seiche-induced mixing: Its impact on lake productivity. *Limnol. Oceanogr.* **41**: 323–332, doi:10.4319/lo.1996.41.2.0323.
- Pannard, A., M. Bormans, and Y. Lagadeuc. 2008. Phytoplankton species turnover controlled by physical forcing at different time scales. *Can. J. Fish. Aquat. Sci.* **65**: 47–60, doi:10.1139/F07-149.
- Platt, T., C. L. Gallegos, and W. G. Harrison. 1980. Photoinhibition of photosynthesis in natural assemblages of marine phytoplankton. *J. Mar. Res.* **38**: 687–701.
- Press, W. H., B. P. Flannery, S. A. Teukolsky, and W. T. Vetterling. 1992. *Numerical Recipes in Fortran 77: The Art of Scientific Computing*. 2nd ed. Cambridge University Press.
- Reynolds, C. S. 2006. *Ecology of Phytoplankton*. Cambridge University Press.
- Reynolds, C. S., V. Huszar, C. Kruk, L. Naselli-Flores, and S. Melo. 2002. Towards a functional classification of the freshwater phytoplankton. *J. Plankton Res.* **24**: 417–428, doi:10.1093/plankt/24.5.417.
- Rimmer, A., I. Ostrovsky, and Y. Yacobi. 2008. Light availability for *Chlorobium phaeobacteroides* development in Lake Kinneret. *J. Plankton Res.* **30**: 765–776, doi:10.1093/plankt/fbn037.
- Rinke, K., I. Hubner, T. Petzoldt, S. Rolinski, M. König-Rinke, J. Post, A. Lorke, and J. Benndorf. 2007. How internal waves influence the vertical distribution of zooplankton. *Freshwater Biol.* **52**: 137–144, doi:10.1111/j.1365-2427.2006.01687.x.
- Robertson, D. M., and J. Imberger. 1994. Lake number, a quantitative indicator of mixing used to estimate changes in dissolved oxygen. *Int. Rev. Hydrobiol.* **79**: 159–176, doi:10.1002/iroh.19940790202.
- Rueda-Valdivia, F., and G. Schladow. 2009. Mixing and stratification in lakes of varying horizontal length scales: Scaling arguments and energy partitioning. *Limnol. Oceanogr.* **54**: 2003–2017, doi:10.4319/lo.2009.54.6.2003.
- Sartory, D., and J. Grobbelaar. 1984. Extraction of chlorophyll *a* from freshwater phytoplankton for spectrophotometric analysis. *Hydrobiologia.* **114**: 177–187, doi:10.1007/BF00031869.
- Schallenberg, M., and C. W. Burns. 2004. Effects of sediment resuspension on phytoplankton production: Teasing apart the influences of light, nutrients and algal entrainment. *Freshwater Biol.* **49**: 143–159, doi:10.1046/j.1365-2426.2003.01172.x.
- Scheffer, M. 2001. Alternative attractors of shallow lakes. *Sci. World J.* **1**: 254–263.
- Søndergaard, M., P. Kristensen, and E. Jeppesen. 1992. Phosphorus release from resuspended sediment in the shallow and wind-exposed Lake Arreso, Denmark. *Hydrobiologia.* **228**: 91–99, doi:10.1007/BF00006480.
- Turner, J. S. 1973. *Buoyancy Effects in Fluids*. Cambridge University Press.
- Vidal, J., F. J. Rueda, and X. Casamitjana. 2007. The seasonal evolution of high vertical-mode internal waves in a deep reservoir. *Limnol. Oceanogr.* **52**: 2656–2667, doi:10.4319/lo.2007.52.6.2656.
- Walsh, P., and L. Legendre. 1983. Photosynthesis of natural phytoplankton under high frequency light fluctuations simulating those induced by sea surface waves. *Limnol. Oceanogr.* **28**: 688–697, doi:10.4319/lo.1983.28.4.0688.
- Wiegand, R. C., and V. Chamberlain. 1987. Internal waves of the second vertical mode in a stratified lake. *Limnol. Oceanogr.* **32**: 29–42, doi:10.4319/lo.1987.32.1.0029.
- Yamamoto, T., and G. Hatta. 2004. Pulsed nutrient supply as a factor inducing phytoplankton diversity. *Ecol. Model.* **171**: 247–270, doi:10.1016/j.ecolmodel.2003.08.011.

Received: 29 March 2010

Amended: 9 November 2010

Accepted: 17 January 2011